RESEARCH ARTICLE

ADVANCED
SENSOR
RESEARCH
Open Access

www.advsensorres.com

Cross-Correlated Quantum Thermometry Using Diamond Containing Dual-Defect Centers

Madhav Gupta, Tongtong Zhang, Lambert Yeung, Jiahua Zhang, Yayin Tan, Yau Chuen Yiu, Shuxiang Zhang, Qi Wang, Zhongqiang Wang, and Zhiqin Chu*

The contactless temperature measurement at micro/nanoscale is vital to a broad range of fields in modern science and technology. The nitrogen-vacancy (NV) center, a kind of diamond defect with unique spin-dependent photoluminescence, is recognized as one of the most promising nanothermometers. However, this quantum thermometry technique is prone to a number of possible perturbations, which will unavoidably degrade its actual temperature sensitivity. Here, for the first time, a cross-validated optical thermometry method is developed using a bulk diamond sample containing both NV centers and silicon-vacancy (SiV) centers, achieving a sensitivity of 22 and 86 mK $(\sqrt{Hz})^{-1}$ respectively. Particularly, the latter has been intrinsically immune to those influencing perturbations for the NV-based quantum thermometry, hence serving as a real-time cross-validation system. As a proof-of-concept demonstration, a trustworthy temperature measurement is shown under the influence of varying magnetic fields, which is a common artefact present in practical systems. This multi-modality approach allows synchronized cross-validation of the measured temperature, which is required for micro/nanoscale quantum thermometry in complicated environments such as a living cell.

1. Introduction

Performing high-resolution thermometry with nanoscale spatial resolution is crucial in studying multiple processes in diverse fields such as electronics, material science, and cell biology.[1–5]

For example, multiple physiological properties in thermal biology are directly revealed by measuring the temperature in biological systems.[6] There are growing interests in developing non-contact luminescent thermometry techniques to explore the measurements of temperature at single cell level.[6,7] Among the different approaches, the optically addressable nitrogen-vacancy (NV) center in diamond nanoparticles remains one of the most studied and well-adopted high-sensitive nanothermometers.[8] The NV center uses a magnetic spin transition whose resonance frequency is sensitive to thermally induced lattice expansion. This spin-based method has exceptionally high sensitivity and has been shown to detect temperature variations down to 9 mK $(\sqrt{Hz})^{-1}$ in pure diamond and 200 mK $(\sqrt{Hz})^{-1}$ in nanodiamonds with a spatial resolution of 200nm.[7] Several exciting applications of this method have been demonstrated, such as nanoscale thermometry in electronic devices,[9] living cells,[7] and C. elegans worms.[10]

However, this spin-based method has been found susceptible to multiple artefacts such as fluctuating magnetic fields,[11] microwave heating,[12,13] and uncontrolled movements.[8,14] In

M. Gupta, T. Zhang, J. Zhang, Y. Tan, Y. C. Yiu, S. Zhang, Z. Chu
Department of Electrical and Electronic Engineering
The University of Hong Kong
Pokfulam Road, Hong Kong SAR, China
E-mail: zqchu@eee.hku.hk

L. Yeung
6C Technology Limited
Dai Hei St, Tai Po, Hong Kong SAR, China

S. Zhang
College of Polymer Science and Engineering, State Key Laboratory of Polymer Materials and Engineering
Sichuan University
Chengdu 610065, China

Q. Wang, Z. Wang
Dongguan Institute of Opto-Electronics
Peking University
Dongguan, Guangdong 523808, China

Z. Chu
School of Biomedical Sciences
The University of Hong Kong
Pokfulam Road, Hong Kong SAR, China

**ADVANCED
SCIENCE NEWS**

www.advancedsciencenews.com

**ADVANCED
SENSOR
RESEARCH**

www.advsensorres.com

addition, the required microwave irradiations lead to considerable residual heating effects and might not be suitable for biological samples such as neuron cells.[15] Due to these practical implementation issues, several microwave-free all-optical approaches have been demonstrated using a series of diamond defects such as NV,[16] silicon-vacancy (SiV),[17,18] germanium vacancy (GeV),[19] and tin vacancy (SnV)[20,21] centers. For instance, temperature measurement within the biological transparency window by the SiV defect in diamonds has been recently reported.[18] Here the temperature sensitivity reached 360 mk $(\sqrt{Hz})^{-1}$ in bulk diamond and 521 mk $(\sqrt{Hz})^{-1}$ in 200 nm nanodiamonds at room temperature. While the all-optical method has been shown to be relatively immune to those measurement artefacts, it suffers from relatively poor sensitivity as compared to the spin-based approach.[8] Notably, most of the existing studies have relied on one single type of defect centers, and only a few recent studies[22,23] have started to demonstrate the case of deploying dual-defects simultaneously in one go.

For reliable temperature measurements in practical applications, it is highly desirable to develop a multi-modality thermometer allowing cross-validation of each individual readout method.[5] Recently, multi-mode temperature measurements have been demonstrated, e.g., Alkahtani et al. reported the simultaneous use of fluorescent nanodiamonds (FNDs) and lanthanide ion-doped upconverting nanoparticles (UCNPs) in fertilized bovine embryos.[22] They injected both FNDs and UCNPs into the embryos, performing Optically Detected Magnetic Resonance (ODMR) measurements for the FNDs, and the fluorescence spectral measurements for the UCNPs aimed at increased measurement confidence. Despite its significance, this dual-mode thermometry has actually consisted of two physically separated systems, which limits the spatial resolution and makes synchronous /simultaneous measurements challenging. Similarly, temperature sensing with NV and Nickel (Ni) diamond color centers excited in the biological transparency window in FND crystals was also recently demonstrated.[23] Unfortunately, both the NV and Ni centers show a quite broad phonon sideband, limiting their temperature sensitivity intrinsically.[23]

In this work, we demonstrate a cross-validated/dual-mode optical thermometry method using NV and SiV defect centers in the same bulk diamond sample, without any loss in spatial or temporal resolution. Temperature measurements will be obtained simultaneously using two different modalities, i.e., thermally induced ODMR spectrum and photoluminescence (PL) spectrum shift, corresponding to NV and SiV centers, respectively. We show that these two measurements have a perfect linear dependency, indicating the confidence of the performed temperature measurement can be significantly improved. Furthermore, we have applied this method to demonstrate reliable thermometry, even in the presence of fluctuating electromagnetic fields that mimics a commonly encountered artefact in practical systems. To the best of our knowledge, this is the first time that people have combined the high-sensitivity spin-based approach (NV) with the artefact-free all-optical approach (SiV) within the same thermometer to perform reliable temperature measurements. Specifically, by simultaneously measuring temperature using two different modalities having different physics, our approach avoids sensor confusion and improves the measurement confidence. This could certainly help in addressing the recent controversy surrounding the interpretation of the heterogeneous temperature distribution in living cells.[24,25]

2. Results

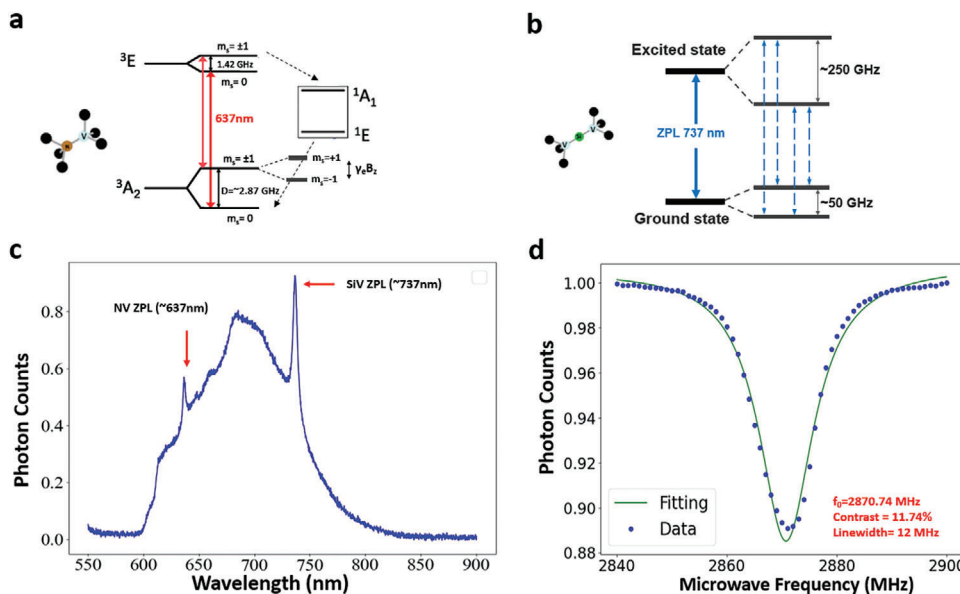### 2.1. Co-Existence of NV and SiV Centers in Diamond

The NV center is a point defect in the diamond lattice, consisting of an adjacent pair of a nitrogen impurity and a lattice vacancy (Inset, **Figure 1**a). The electronic energy level structure of the NV centers is shown in Figure 1a, consisting of spin-1 system ($S = 1$) with a triplet ground state ($^3A_2$) having electron sublevels of $m_S = 0$ and $m_S = \pm 1$. By applying the microwave resonance to the transition between $m_S = 0$ and $m_S = \pm 1$ in the ground state, the fluorescence decreases substantially—and this process is called ODMR.[8] ODMR measurements can be performed to measure the Zero Field Splitting (D), which is equal to $D \approx 2.87$ GHz at room temperature. NV-ODMR based thermometry is based on the temperature dependence of D, originating from thermal expansion of the diamond lattice and the temperature dependence of the electron–phonon interaction.[16,26]

The SiV center is formed by replacing two neighboring carbon atoms in the diamond lattice with one Silicon atom, which places itself between the two vacant lattice sites (Inset, Figure 1b). The electronic energy level structure of the SiV centers is shown in Figure 1b, consisting of doubly degenerate ground and excited orbital states split by spin-orbit coupling.[27] All four transitions between the two ground and two excited orbital states are dipole allowed with a sharp zero phonon line (ZPL) at 737 nm (1.68 eV)[28,29] and a minimal phononic sideband in a roughly 20 nm window ≈ 766 nm.[30] SiV based thermometry is based on the temperature dependence of the ZPL parameters such as peak position and linewidth.

The SiV center emits much more of its emission into its ZPL, $\approx 70\%$ (Debye Waller Factor (DWF) ≈ 0.7) as compared to the NV center (0.04).[31] Moreover, the ZPL is in the Near Infrared Region (NIR) and lies in the biological transparency window. Furthermore, due to the $S = 1/2$ nature of the electron spin and the large ground state energy splitting (50 GHz), the SiV remains largely unaffected by the magnetic field at room temperature.[8] These factors make the SiV center an attractive candidate for a variety of ultrasensitive all-optical thermometry-based applications.[32,33]

A detailed optical characterization for our bulk diamond sample using our custom-built wide-field quantum diamond microscope is performed (see Figure S1, Supporting Information), by measuring the PL spectrum and Continuous Wave (CW)–ODMR spectrum to experimentally confirm the coexistence of dual defect centers. Figure 1c shows the PL spectrum measured at 25 °C under 532 nm excitation. The ZPL peaks of NV and SiV at 637 and 737 nm respectively can be clearly observed, indicating their coexistence.

By performing the appropriate Lorentzian fitting, the linewidths for the NV and SiV ZPL peaks are extracted as ≈ 3 and ≈ 4.8 nm respectively, which are in close agreement with values reported for a typical 1b diamond at room temperature.[34] Additionally, a standard CW-ODMR spectrum measurement at 25 °C is also performed (Figure 1d) that further confirms the presence of an ensemble of NV centers in the bulk diamond

ADVANCED
SCIENCE NEWS

www.advancedsciencenews.com

ADVANCED
SENSOR
**RESEARCH**
Open Access

www.advsensorres.com

Figure 1. a) Energy level diagram and atomic structure of the NV center. The inset shows the NV center crystal structure b) Energy level diagram and atomic structure of the SiV defect center. The inset shows the SiV crystal structure c) PL spectrum of sample at 25 °C, inset is a typical photo of our customized diamond sample. d) Typical Continuous Wave (CW)-ODMR spectrum at 25 °C with the relevant parameters extracted from Lorentzian Data fitting.

sample. A Lorentzian data fitting is performed to extract the ODMR contrast (11.74%) and linewidth (12 MHz). Interestingly, the ODMR measurement is performed successfully under the influence of the SiV fluorescence as a background signal (with a 650 nm longpass filter).

This demonstrates the mutual independence of the two methods and shows no significant crosstalk between the two defect centers in the diamond sample. This is consistent with recent literate reports about the coexistence of two defect centers in the same bulk diamond sample.[35] A material characterization of the bulk diamond sample used is also provided in the Supporting Information (X-Ray Diffraction (XRD)/Raman measurements are shown in Figure S2, Supporting Information), indicating the high crystalline quality of our sample. Additional mea-

surements need to be performed to quantitatively estimate the exact NV/SiV concentrations in the bulk diamond sample.

Apart from the PL and ODMR measurements, the performance of the two thermometry methods also need to be characterized, to confirm whether the co-existence of the two defect centers in the sample has any adverse effects on the sensitivity. The photostability of the sample was measured by recording photon counts under 532 nm excitation for over 30 min at 25 °C, and a deviation of <0.41% was measured (**Figure 2**a). To estimate the precision of SiV thermometry, we measure the uncertainty (standard deviation) in the ZPL peak position as a function of integration time at a fixed temperature of 25 °C (Figure 2b). The linear fitting with a negative slope = −0.5, corresponds to the theoretical shot-noise limit[8] $\sigma_T \propto \sqrt{t}$, where the proportionality constant is the
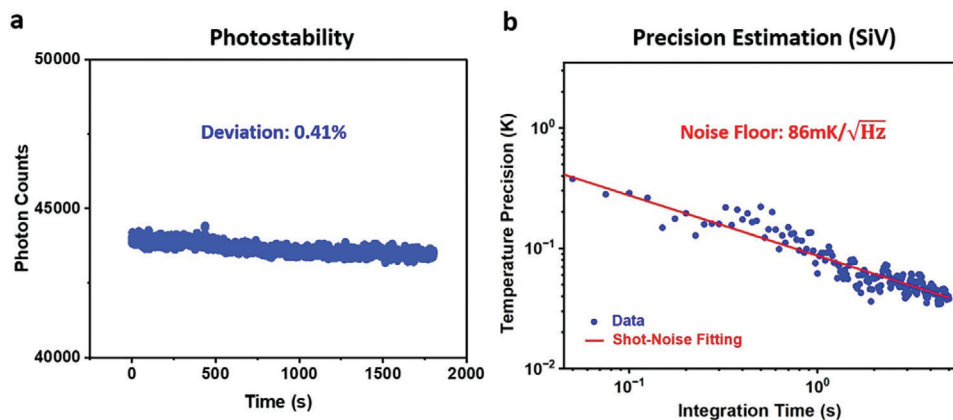
Figure 2. a) The monitored time-trace of fluorescence in diamond sample for a period of 30 min. The photon counts are measured for an exposure time of 10 ms and averaged over 400 pixels. b) The measured temperature precision of the all-optical SiV-based temperature measurement as a function of integration time. A noise floor of 86 mK $(\sqrt{Hz})^{-1}$ is extracted from the shot-noise fitting.
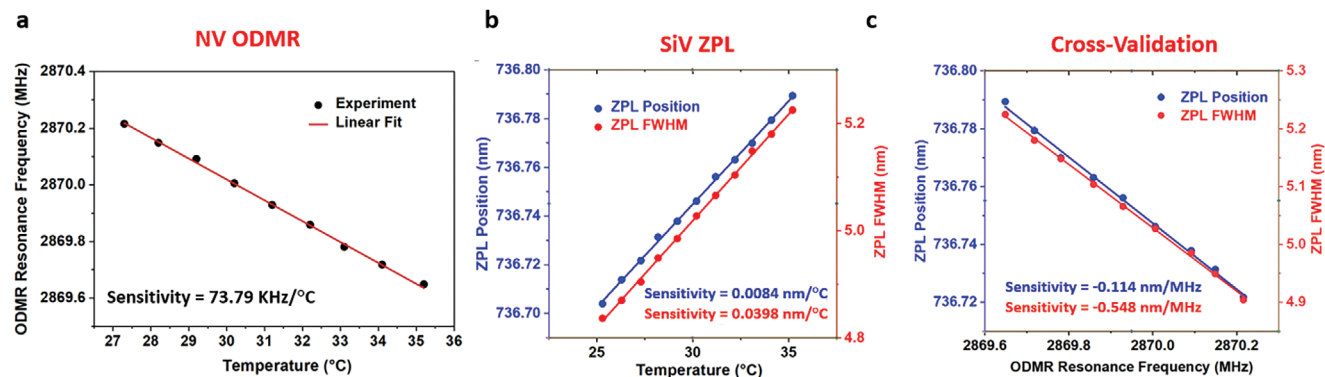
Figure 3. a) ODMR Resonance Frequency is measured as a function of temperature, and a thermal susceptibility of 73.79 kHz °C⁻¹ is extracted. b) The SiV ZPL position and FWHM are measured as a function of temperatures, and thermal susceptibilities of 0.0084 and 0.0398 nm °C⁻¹ are extracted respectively. c) The SiV ZPL Position/FWHM measurement is shown as a function of NV-ODMR resonance frequency. Error bars represent the standard deviation calculated from 10 individual measurements. Error bars for a–c) are smaller than the size of the datapoint.

noise floor $\eta_T = 86$ mK $(\sqrt{Hz})^{-1}$. Similarly, to estimate the precision of NV-ODMR based thermometry, a Lorentzian Data-fitting on the CW-ODMR spectrum is performed to extract the contrast and linewidth, and then the well-known theoretical relation[8] is used to calculate a sensitivity of 22 mK $(\sqrt{Hz})^{-1}$ (see Supporting Information). The measured noise floors for both methods are comparable to the sensitivities reported in previous works.[8]

2.2. Cross-Validated Temperature Measurement

Temperature measurements are demonstrated by measuring the NV-ODMR resonance frequency, SiV ZPL parameters (Peak Position, Peak Full Width Half Maximum (FWHM)) as a function of diamond sample temperature. At each temperature, the ODMR and PL Spectrum measurements are performed, and the parameters mentioned above are extracted by performing the relevant Data fitting. The temperature of the diamond sample was stabilized using an electronic temperature-controlled system (global heating source), having a precision of 0.1 °C.

Figure 3a demonstrates NV-ODMR based thermometry where the resonance frequency is measured as a function of temperature, and a strong linear dependence is observed. A susceptibility of 73.79 kHz °C⁻¹ is derived from linear fitting, which closely matched previously reported values.[8] Similarly, Figure 3b demonstrates all-optical SiV-based temperature measurement where the ZPL Peak position and FWHM are shown to have a strong linear dependence on temperature, and the susceptibilities are derived from the corresponding linear fitting. The key result of our project is shown in Figure 3c, where the temperature measurement is performed simultaneously using the NV-ODMR and SiV-ZPL shift-based methods. The accurate linear relationship between the ODMR resonance frequency and SiV ZPL position provides strong evidence that the two independent mechanisms can be used to cross-validate each other simultaneously and synchronously.

Additionally, we further demonstrate cross validation temperature measurements by using the excitation laser (532 nm) as a local heating source. The NV ODMR resonance frequency and SiV ZPL peak position are measured simultaneously as a function

of laser power, in both the static and dynamic settings (Figure S3, Supporting Information). A close agreement between the 2 temperature measurement methods is found, which practically demonstrates how the all-optical SiV ZPL measurements can be used to verify the spin-based NV ODMR measurements in a stable and repeatable manner. (See Supporting Information for experimental details). After demonstrating the viability and feasibility of our cross-validation approach, we explore a practical application of this method in the next section.

2.3. Practical Application of the Developed Cross-Validated Method

The main driving force of this project is that the NV-ODMR measurement is susceptible to multiple artefacts such as external fluctuating electromagnetic fields, microwave-induced heating, etc. This hampers the quality of the measurements and inevitably reduces the accuracy and reliability of the measurement performed. As a comparison, the SiV-based temperature method is all-optical, and is immune to the above-mentioned artefacts.

As a proof-of-concept demonstration, we study the effect of a randomly oriented dynamic magnetic field as a measurement artefact for NV ODMR-based measurement. The applied B field is applied manually by the experimenter and fluctuates randomly both in magnitude and direction, with a typical frequency on the order of Hz. This mimics a common measurement artefact (fluctuating electromagnetic fields) found in many systems, e.g., in complex biological environments such as neuron cells and cardiac tissues.[36] While it is possible to accurately measure temperature in the presence of magnetic noise (and vice versa) either by using multi-point methods[6] or by performing a mathematical analysis on the fitted resonance frequencies,[8,9] these methods only work if the B field can be assumed to be static during the measurement time of the ODMR spectrum.

Figure 4a,b demonstrates how an external magnetic field leads to the splitting of the ODMR spectrum, resulting in a lower contrast and a higher linewidth. These factors lead to a degraded temperature sensitivity for the NV based ODMR measurement. As a proof-of-concept demonstration, we measure the ODMR
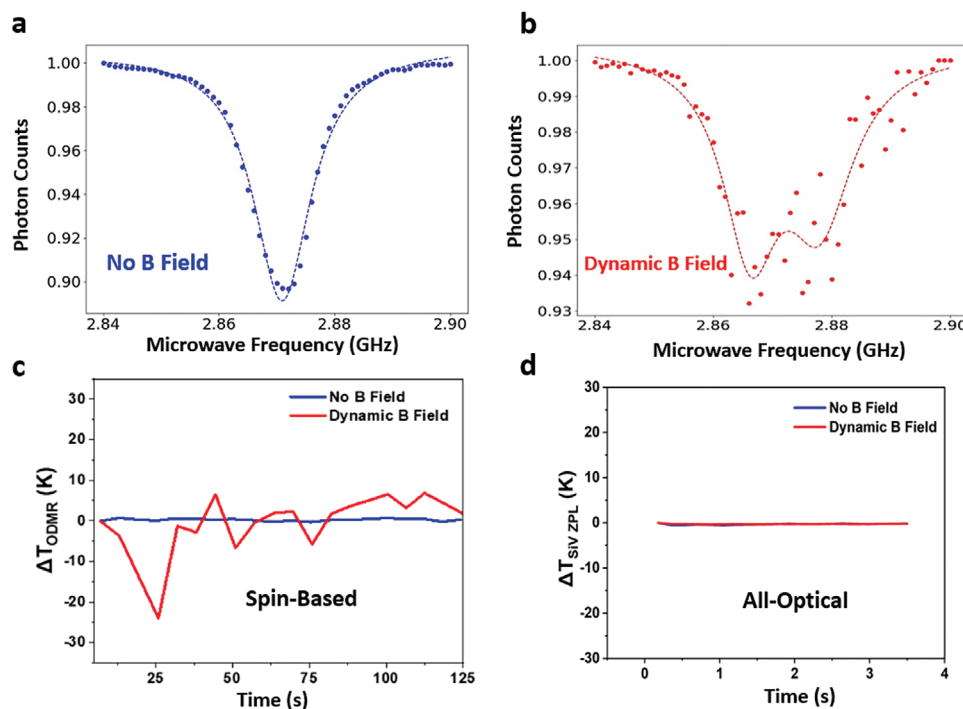
Figure 4. a) Influence of dynamic magnetic fields on the ODMR-based diamond thermometry. a) CW-ODMR spectra shown absence of B field. b) CW-ODMR spectra in the presence of randomly oriented dynamic B field c) Time trace of measured temperature change for NV-ODMR based method. d) Time-trace of measured temperature change for all-optical SiV ZPL based method.

resonance frequency as a function of time (Figure 4c), both in the presence and absence of an external fluctuating magnetic field. As expected, the measured temperature change has a large variance and standard deviation when a dynamic external magnetic field is applied. On the contrary, when the same temperature measurement is performed for the all-optical SiV-based spectrum parameters (Figure 4d), there is comparably a significantly lower variance when an external magnetic field is applied. This demonstrates how the SiV-based method can be used to validate the NV-based ODMR method in the presence of measurement artefacts, as shown for fluctuating magnetic fields.

3. Conclusion

In this letter, we have proposed that it is feasible to effectively combine the high sensitivity, accuracy, and stability of NV-ODMR measurement, with the advantages of artefact-free all-optical SiV approach, without any loss in spatial or temporal resolution, to improve the reliability and measurement confidence of temperature measurements. We envision a variety of novel applications in the future by combining multiple defect centers in the same diamond sample, simultaneously utilizing the advantages and usecases of different color centers together.

For example, dual-defect centers can allow us to decouple the Temperature (T) and B field measurements, significantly simplifying the measurement and making it more reliable. Simultaneous T and B measurements have multiple applications and have been performed multiple times before.[8,9] However, this involves mathematical calculations on the multiple extracted resonance frequencies and can only be accurately and reliably done when

T and B are both assumed to be static during the time taken to perform the measurement. Using dual-mode quantum sensing, i.e., SiV for T measurements and NV for B-field measurement, allows us to make precise magnetic field measurements in the presence of temperature fluctuations and vice versa.

Furthermore, while the current measurements were performed on a bulk diamond sample that might limit the scope of its practical applications, we propose a sample fabrication procedure to obtain nanodiamonds containing dual defect centers. That would allow cross-validation of temperature measurement with a nanoscale spatial resolution. The nanodiamond sample fabrication procedure has been described in the Supporting Information, and preliminary experimental results are shown in Figure S4 (Supporting Information). The detection of simultaneous NV and SiV ZPL peaks in the PL Spectrum measurement indicates the co-existence of both defect centers in a single nanodiamond. Further sample optimization is required in order to improve the Signal-to-noise Ratio (SNR) of the ZPL peaks, following that a detailed characterization of the sensitivity and performance for the nanodiamond case can be performed. Moreover, performing a ball milling process on the currently used bulk diamond sample[37] shall also yield nanodiamonds having a coexistence of NV and SiV.

In conclusion, in this work, we have succeeded in measuring temperature simultaneously using two independent mechanisms (NV-ODMR and SiV-ZPL) without any substantial loss in sensitivity or temporal resolution. The use of two modalities enables cross-validation and makes these results far more reliable for nanothermometers in complex systems such as living cells.

Supporting Information

Supporting Information is available from the Wiley Online Library or from the author.

Acknowledgements

Conflict of Interest

The authors declare no conflict of interest.

Keywords

[1] T. Zhang, G. Pramanik, K. Zhang, M. Gulka, L. Wang, J. Jing, F. Xu, Z. Li, Q. Wei, P. Cigler, Z. Chu, *ACS Sens.* **2021**, *6*, 2077.

[2] R. Schirhagl, K. Chang, M. Loretz, C. L. Degen, *Annu. Rev. Phys. Chem.* **2014**, *65*, 83.

[3] M. W. Doherty, N. B. Manson, P. Delaney, F. Jelezko, J. Wrachtrup, L. C. Hollenberg, *Phys. Rep.* **2013**, *528*, 1.

[4] T. Muller, C. Hepp, B. Pingault, E. Neu, S. Gsell, M. Schreck, H. Sternschulte, D. Steinmuller-Nethl, C. Becher, M. Atature, *Nat. Commun.* **2014**, *5*, 3328.

[5] <number>[5]</numsber>H. Precht, J. Christophersen, H. Hensel, W. Larcher, in *Temperature and Life*, Springer, Berlin **1973**.

[6] J. Zhou, B. del Rosal, D. Jaque, S. Uchiyama, D. Jin, *Nat. Methods* **2020**, *17*, 967.

[7] G. Kucsko, P. Maurer, N. Yao, M. Kubo, H. Noh, P. Lo, H. Park, M. Lukin, *Nature* **2013**, *500*, 54.

[8] M. Fujiwara, Y. Shikano, *Nanotechnology* **2021**, *32*, 482002.

[9] C. Foy, L. Zhang, M. E. Trusheim, K. R. Bagnall, M. Walsh, E. N. Wang, R. Englund, *ACS Appl. Mater. Interfaces* **2020**, *12*, 26525.

[10] M. Fujiwara, S. Sun, A. Dohms, Y. Nishimura, K. Suto, Y. Takezawa, K. Oshimi, L. Zhao, N. Sadzak, Y. Umehara, Y. Teki, N. Komatsu, O. Benson, Y. Shikano, E. Kage-Nakadai, *Sci Adv.* **2020**, *6*, eaba9636.

[11] H. Clevenson, E. H. Chen, F. Dolde, C. Teale, D. Englund, D. Braje, *Phys. Rev. A* **2016**, *94*, 021401.

[12] P. Andrich, J. Li, X. Liu, F. J. Heremans, P. F. Nealey, D. Awschalom, *Nano Lett.* **2018**, *18*, 4684.

[13] Z. Wang, J. Zhang, X. Feng, L.i Xing, *ACS Omega* **2022**, *7*, 31538.

[14] Y. Nishimura, K. Oshimi, Y. Umehara, Y. Kumon, K. Miyaji, H. Yukawa, Y. Shikano, T. Matsubara, M. Fujiwara, *Sci. Rep.* **2021**, *11*, 4248.

[15] J. P. Nguyen, F. B. Shipley, A. N. Linder, G. S. Plummer, M. Liu, S. U. Setru, J. W. Shaevitz, A. M. Leifer, *Proc. Natl. Acad. Sci. USA*, **2016**, *113*, E1074.

[16] T. Plakhotnik, M. W. Doherty, J. H. Cole, R. Chapman, N. B. Manson, *Nano Lett.* **2014**, *14*, 4989.

[17] S. Choi, V. Agafonov, V. Davydov, T. Plakhotnik, *ACS Photonics* **2019**, *6*, 1387.

[18] C. T. Nguyen, R. E. Evans, A. Sipahigil, M. K. Bhaskar, D. D. Sukachev, V. N. Agafonov, V. A. Davydov, L. F. Kulikova, F. Jelezko, D. Lukin, *Appl. Phys. Lett.* **2018**, *112*, 203102.

[19] J.-W. Fan, I. Cojocaru, J. Becker, I. V. Fedotov, M. H. A. Alkahtani, A. Alajlan, S. Blakley, M. Rezaee, A. Lyamkina, Y. N. Palyanov, Y. M. Borzdov, Y.a-P. Yang, A. Zheltikov, P. Hemmer, A. V. Akimov, *A. C. S. Photonics* **2018**, *5*, 765.

[20] S. Ditalia Tchernij, T. Lühmann, T. Herzig, J. Küpper, A. Damin, S. Santonocito, M. Signorile, P. Traina, E. Moreva, F. Celegato, S. Pezzagna, I. P. Degiovanni, P. Olivero, M. Jaksič, ´J. Meijer, P. M. Genovese, J. Forneris, *ACS Photonics* **2018**, *5*, 4864.

[21] M. Alkahtani, I. Cojocaru,X. Liu, T. Herzig, J. Meijer, J. Kupper, T. Luhmann, A. V. Akimov, P. R. Hemmer, *Appl. Phys. Lett.* **2018**, *112*, 241902.

[22] M. Alkahtani, L. Jiang, R. Brick, P. Hemmer, M. Scully, *Opt. Lett.* **2017**, *42*, 4812.

[23] M. H. Alkahtani, F. Alghannam, L. Jiang, A. A. Rampersaud, R. Brick, C. L. Gomes, M. O. Scully, P. R. Hemmer, *Opt. Lett.* **2018**, *43*, 3317.

[24] M. Suzuki, T. Plakhotnik, *Biophys. Rev.* **2020**, *12*, 593.

[25] S. Ghonge, D. C. Vural, *J. Stat. Mech.* **2018**, *7*, 073102.

[26] X.-D. Chen, C.-H. Dong, F.-W. Suna, C.-L. Zou, J.-M. Cui, Z.-F. Han, G.-C. Guo, *Appl. Phys. Lett.* **2011**, *99*, 161903.

[27] B. Pingault, D.-D. Jarausch, C. Hepp, L. Klintberg, J. N. Becker, M. Markham, *Nat. Commun.* **2017**, *8*, 15579.

[28] Y. Liu, G. Chen, Y. Rong, L. P. McGuinness, F. Jelezko, S. Tamura, T. Tanii, T. Teraji, S. Onoda, T. Ohshima, J. Isoya, T. Shinada, E. Wu, H. Zeng, *Sci. Rep.* **2015**, *5*, 12244.

[29] T. Feng, B. D. Schwartz, *J. Appl. Phys.* **1993**, *73*, 1415.

[30] A. Dietrich, K. D. Jahnke, J. M. Binder, T. Teraji, J. Isoya, L. J. Rogers, F. Jelezko, *New J. Phys.* **2014**, *16*, 113019.

[31] I. Aharonovich, S. Castelletto, D. A. Simpson, C.-H. Su, A. D. Greentree, S. Prawer, *Rep. Prog. Phys.* **2011**, *74*, 076501.

[32] T. Zhang, M. Gupta, J. Jing, Z. Wang, X. Guo, Y.e Zhu, Y. C. Yiu, T. K. C. Hui, Q.i Wang, K. H. Li, Z. Chu, *J. Mater. Chem. C* **2022**, *10*, 13734.

[33] W. Liu, M.d N. A. Alam, Y. Liu, V. N. Agafonov, H. Qi, K. Koynov, V. A. Davydov, R. Uzbekov, U. Kaiser, T. Lasser, F. Jelezko, A. Ermakova, T. Weil, *Nano Lett.* **2022**, *22*, 2881.

[34] B. Dong, C. Shi, Z. Xu, K. Wang, H. Luo, F. Sun, P. Wang, E. Wu, K. Zhang, J. Liu, Y. Song, Y.e Fan, *Diamond Relat. Mater.* **2021**, *116*, 108389.

[35] L. Golubewa, Y. Padrez, S. Malykhin, T. Kulahava, E. Shamova, I. Timoshchenko, M. Franckevicius, A. Selskis, R. Karpicz, A. Obraztsov, Y. Svirko, P. Kuzhir, *Adv. Opt. Mater.* **2022**, *10*, 2270060.

[36] K. Arai, A. Kuwahata, D. Nishitani, I. Fujisaki, R. Matsuki, Y. Nishio, Z. Xin, X. Cao, Y. Hatano, S. Onoda, C. Shinei, M. Miyakawa, T. Taniguchi, M. Yamazaki, T. Teraji, T. Ohshima, M. Hatano, M. Sekino, T. Iwasaki, *Commun. Phys.* **2022**, *5*, 200.

[37] C. R. Lin, D. H. Wei, M. K. B. Dao, R. J. Chung, M. H. Chang, *Appl. Mech. Mater.* **2013**, *284-287*, 168.